PROCEEDINGS OF SPIE

SPIEDigitalLibrary.org/conference-proceedings-of-spie

Large-area electronic skins in space: vision and preflight characterization for first aerospace piezoelectric e-textile

Cherston, Juliana, Veysset, David, Sun, Yuchen, Yano, Hajime, Nelson, Keith, et al.

Juliana Cherston, David Veysset, Yuchen Sun, Hajime Yano, Keith A. Nelson, Shobha Murari, Joseph A. Paradiso, "Large-area electronic skins in space: vision and preflight characterization for first aerospace piezoelectric e-textile," Proc. SPIE 11379, Sensors and Smart Structures Technologies for Civil, Mechanical, and Aerospace Systems 2020, 113791Q (23 April 2020); doi: 10.1117/12.2557942

SPIE. Event: SPIE Smart Structures + Nondestructive Evaluation, 2020, Online Only, California, United States

Downloaded From: https://www.spiedigitallibrary.org/conference-proceedings-of-spie on 13 May 2020 Terms of Use: https://www.spiedigitallibrary.org/terms-of-use

Large-Area Electronic Skins In Space: Vision and Preflight Characterization For First Aerospace Piezoelectric e-Textile

Juliana Cherston[a], David Veysset[e], Yuchen Sun[b,e], Hajime Yano[c], Keith A. Nelson[b,e], Shobha Murari[d], and Joseph A. Paradiso[a]

[a]MIT Media Lab Responsive Environments Group, 75 Amherst Street, Cambridge MA, USA
[b]Department of Chemistry, MIT, Cambridge, 02139, Massachusetts, USA
[c]JAXA Institute of Space and Astronautical Science (ISAS) 3-1-1 Yoshinodai, Chuo-ku, Sagamihara City, Kanagawa Prefecture, Japan 252-5210
[d]JPS Composite Materials, 2200 S Murray Ave, Anderson, South Carolina, 29622
[e]Institute for Soldier Nanotechnologies, Massachusetts Institute of Technology, 77 Massachusetts Avenue, Cambridge, MA 02139, USA

ABSTRACT

Aerospace-grade textiles have decades of flight heritage for protection against harsh elements of the space environment. However, these substrates have remained electrically passive despite occupying useful large-area real-estate on the exterior walls of persistent spacecraft. By leveraging electronic textiles in an aerospace context, hybrid fabrics can be developed that simultaneously protect spacecraft while also detecting debris or micrometeoroid hypervelocity impactors. Specifically, this paper describes prototype development and preflight testing of piezoelectric Beta cloth ahead of a scheduled late 2020 material resiliency test on the International Space Station. Two accessible manufacturing methods for piezoelectric fiber are introduced based on modifications to piezoelectric cable that reduce diameter, increase mechanical flexibility of the fiber, and improve compatibility with textile weft insertion techniques. A Beta cloth simulant with piezoelectric fiber is introduced and custom ultra low power readout electronics are specified, which allow for a first-order power consumption estimate for scaling of this material across large-area spacecraft walls. Finally, high-velocity impact sensor data measured using the Laser Induced Particle Impact Test (LIPIT) facility is presented, building towards an accurate prediction of impactor velocity.

1. INTRODUCTION

1.1 Prelude: 'Sensate Fabric for the Cosmos'

Humanity's instinctive will to explore draws modern civilization towards evermore extreme environments, sustained by a hunger for radical and direct sensory experience, as well as a conviction to comprehend the fundamental nature of things on Earth and beyond. Alas, until it is possible to substantially alter the human body, the humble textile will continue to serve as a boundary - a second skin - for the arctic explorer, for the deep-sea diver, and indeed for the astronaut. The textile will also continue to operate as core foundational infrastructure - the likes of tethers, ropes, nets, and habitat skins - that enable and sustain our journey.

Woven substrates have long served as protective agents against harsh environments on Earth, ranging from human-scale, thermally resilient fabric preventing firefighters from overheating[1] to kilometer-scale, high-stiffness geotextiles ensuring that land embankments remain stable.[2] The textile's mechanical flexibility, myriad achievable material properties, and ease of manufacturing at scale uniquely precondition it to certain feats of engineering.

Humanity now endeavors to establish a more significant presence in Low Earth Orbit and beyond. Broadly underpinning the work described here is a fresh avenue for inquiry: what unique experiences and modes of

Further author information: (Send correspondence to)
Juliana Cherston: E-mail: cherston@mit.edu

Sensors and Smart Structures Technologies for Civil, Mechanical, and Aerospace Systems 2020
edited by Haiying Huang, Hoon Sohn, Daniele Zonta, Proc. of SPIE Vol. 11379, 113791Q

© 2020 SPIE CCC code: 0277-786X/20/$21

· doi: 10.1117/12.2557942

Downloaded From: https://www.spiedigitallibrary.org/conference-proceedings-of-spie on 13 May 2020
Terms of Use: https://www.spiedigitallibrary.org/terms-of-use

scientific data collection might be enabled by advancing the electrically passive aerospace-grade textile found on habitats, spacesuits, and spacecraft tethers into a *multifunctional, electroactive, and scalable sensate medium?*

For the first time, we are leveraging electronic textiles in space, the ultimate frontier for exploration where large area protective fabrics have decades of flight heritage.[*] To this end, in 2020, we will be launching the first suite of electronic textile samples to the ExHAM external exposure facility on the International Space Station for initial material resilience testing. An emphasis on hypervelocity impact detection (as initially conceptualized in [3]) sets the stage for the breadth of additional possible functions for a sensate textile in space - from pressurized spacesuit skins that detect external touch, to tension-sensing spacecraft tethers.

1.2 Multifunctional Aerospace Textiles

While specialized fabrics have historically remained passive and unifunctional, the possibility has periodically been raised to integrate sensors and actuators directly into personal protective equipment in order to sense and respond to harsh environments on Earth (see for instance [4] and [5]). This prior work serve as a natural launch point for leveraging electronic textile technology in an aerospace context, where it is crucial to preserve the protective and structural primary functions of the textile even while integrating secondary sensing capabilities.

Note that there is no strict need for this secondary function to relate directly to the primary. In a single substrate, opportunities exist to deeply unify the infrastructure demands and desires of the explorer with the architectures that enable scientific inquiry. For instance, in previous work we proposed the use of fibrous nets that grapple to low gravity bodies, a topology that might serve equally as foundational infrastructure for roving scientific sensor networks and large area solar panels as it does handholds for future space faring explorers.[6,7] By adopting multifunctional design paradigms, scientific experiments may increasingly 'piggy-back' on critical spacecraft submodules in a similar spirit to how e.g. today's CubeSats piggyback off of large spacecraft launches using secondary payload adapter (ESPA) rings.

Historically, the term 'smart skin' has been used in an aerospace context in reference to rigid composite laminates.[8] Described here is a piezoelectric Beta cloth fabric prototype - a smart material initially proposed in [3] that can help to protect and sustain a future tourist's space habitat while also aiding scientists by characterizing sub-millimeter impactors. Broadly, it is a cousin to JAXA's CLOTH Smart Multi-Layer Insulation (MLI) concept in which commercial PVDF film is inserted into an inner layer of conventional MLI.[9] However, these are continuous sheets as opposed to a sensate weaves. SpaceSkin draws from the multidiscplinary field of electronic textile design, which poses unique development and testing challenges. Piezoelectric fibers have yet to be considered or tested in a space environment. Unlike MLI internal layers, the fabric substrate is directly exposed to space, so any design must be demonstrated as both robust to the environment and compatible with industrial weaving processes.

1.3 SUB-MILLIMETER DUST

Ground radar can only track orbital elements at roughly 10 cm diameter or larger. Both the CLOTH and SpaceSkin projects allow for impactors smaller than this threshold to be sensed over a large surface area. Further, the sensate skin can be used on any space mission willing to adopt a modified, multifunctional MLI material, with potential for high adoption rates since MLI is already a required subsystem.

For spacecraft deployed outside of the orbital plane of the planets, interstellar debris dominates - messengers from the depths of space that are regularly passing through our solar system. According to the Panspermia hypothesis,[10] so called 'space dust' may have delivered the organic constituents of life - or potentially microorganisms themselves - to Earth. Therefore, estimating the organic content of impactors using a suite of on-textile sensors is an ambitious ultimate vision.

In the shorter term, high adoption rates among spacecraft deployed in Low Earth Orbit will lead to large datasets that can validate models for dust mass, velocity, and spatial distribution. Further, density approximations can be used to discriminate between human orbital debris and natural micrometeoroids, and potentially be used to estimate the dominant constituent element of the impactor.

Downloaded From: https://www.spiedigitallibrary.org/conference-proceedings-of-spie on 13 May 2020
Terms of Use: https://www.spiedigitallibrary.org/terms-of-use

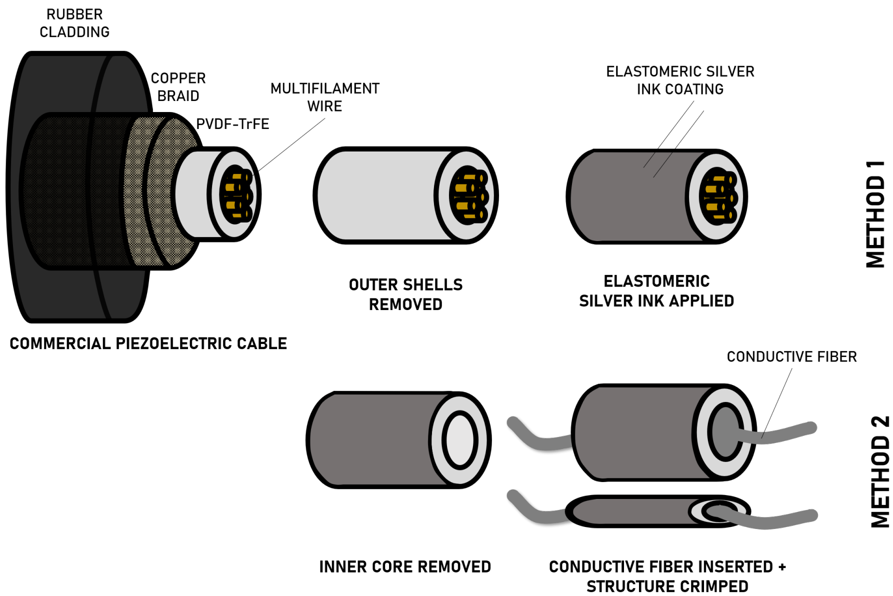

Figure 1. Summary of key piezoelectric fiber prototyping methods developed by modifying commercial piezoelectric cable for compatibility with conventional fabric manufacturing procedures. (In addition, a custom thermally drawn piezoelectric fiber is also under study.)

Method	d_{33} (pC/N)	Bend Radius (cm)	Resistance (Ω/cm)
Commercial	-31 ± 5	5	0.8 ± 0.5
Method 1: SpaceSkin Coated Fiber	-33 ± 5	2	2.4 ± 0.6
Method 2: SpaceSkin Crimped Bead	-9 ± 5	1	2.4 ± 0.6

Table 1. Summary of approximate d_{33}, bend radius, and outer electrode resistance for modified piezoelectric cable manufacturing methods as compared to commercial product

2. PROTOTYPE DEVELOPMENT

2.1 Piezoelectric Cable Development and Specification

Piezoelectric materials demonstrate electromechanical coupling due to noncentrosymetric crystalline structures in e.g. quartz or due to beta-phase dipole alignment in semicrystalline polymers. We have previously provided a brief introduction to ferroelectrics as derived from Gibbs free energy in [3].

Commercially available geometries are generally only available as disks, thin films, cubes, and bulky cabling. However, thin, flexible piezoelectric multilayer fibers have recently been developed in specialized chemistry and materials science laboratories using a variety of precision multimaterial fiber extrusion techniques[11–14] but at present are neither commercialized nor proven to be scalable. In an effort to broaden access to this versatile fiber sensor across a wider range of disciplines and research institutes (human computer interaction laboratories, advanced concept prototyping teams, etc), two related manufacturing methods for piezoelectric fiber have been developed that are more immediately accessible (as summarized in Figure 1). Specifically, these prototyping methods consist of modifying bulky commercial piezoelectric cables for compatibility with conventional electronic loom weft insertion techniques. In each case, the resulting piezoelectric electromechanical coupling coefficient (d_{33} in the plane parallel to the polarization axis) is measured using a quasi-stable Berlincourt d_{33} meter from PolyK Technologies, with one probe connected via wire to the fiber's inner conductive core as depicted in Figure 2.

Method 1: SpaceSkin Coated Fiber The outer rubber shielding and outer copper braiding are removed using precision wire strippers, leaving an inner copper wire core and poled PVDF-TrFE cladding. The

*For an initial presentation of the "SpaceSkin" concept, see [3], 2019).

Downloaded From: https://www.spiedigitallibrary.org/conference-proceedings-of-spie on 13 May 2020
Terms of Use: https://www.spiedigitallibrary.org/terms-of-use

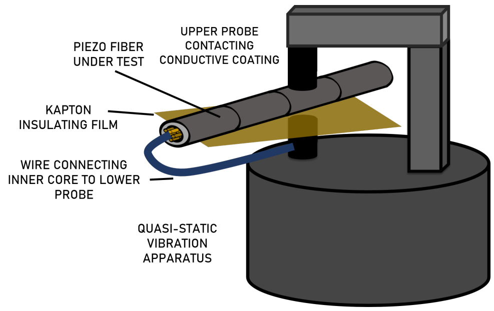

Figure 2. Configuration for measuring rough piezoelectric d_{33} coefficient using fiber rather than conventional thin film sample

PVDF-TrFE cladding is subsequently coated in conductive elastomeric ink CI-1036 from Engineered Conductive Materials (EMS) and cured on a hotplate for 12 hours at 90°C to form an outer conductor. By curing well below the Curie temperature for PVDF-TrFE, no measurable depoling of the activated inner core is detected. Using this approach, fibers of arbitrary lengths can be manufactured with a bend radius measured at roughly 3 cm and d_{33} measured at roughly -33 pC/N, comparable with the original product.

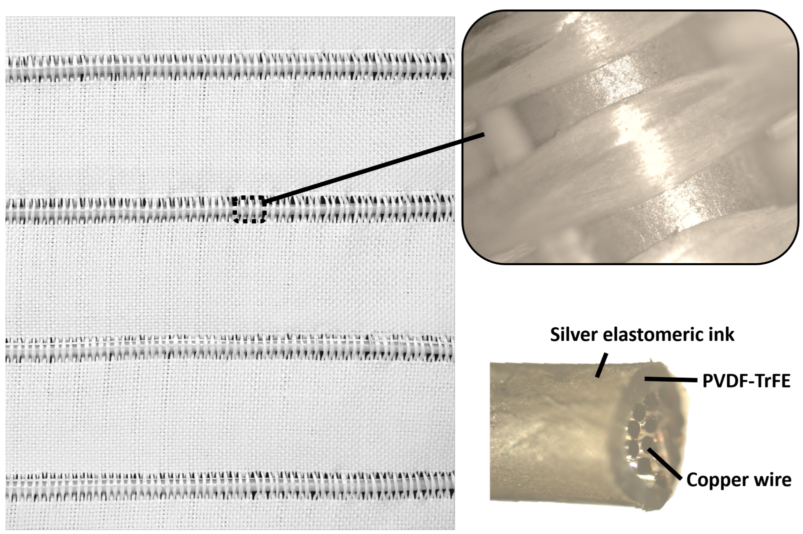

Figure 3. Modification of piezoelectric cabling used in production of sensate Beta cloth substrate

Method 2: SpaceSkin Crimped Bead A viable extension to this method includes removing the inner copper multifilament core, threading in conductive yarn, and using a press to evenly crimp the active piezoelectric element around the yarn, forming a ribbon structure with a conductive core. Due to high friction between the inner wire core and piezoelectric cladding in commercially available products, this method can only be used to manufacture fibers <6 inches in length, but with the benefit of an increased bend radius measured at roughly 1 cm and the ability to crimp multiple short active elements along a single inner conductive yarn core if so desired. However, by modifying the fiber's concentric geometry and disordering the beta-aligned crystalline structure when crimping the prepoled active element, the d_{33} coefficient is reduced to approximately -9 pC/N.

From significant previous prototyping effort as documented [3] and summarized in Table 2, the modification to piezoelectric cable described in Method 1 above is found to be the best available prototyping option short of extruding custom multimaterial fibers with specialized equipment. It is a versatile approach that produces fibers with enough mechanical flexibility and a small enough geometric cross section to be cleanly weft inserted into a textile substrate. Concurrent to introducing this widely accessible manufacturing effort, we are also working

Downloaded From: https://www.spiedigitallibrary.org/conference-proceedings-of-spie on 13 May 2020
Terms of Use: https://www.spiedigitallibrary.org/terms-of-use

	Manufacturable		Poleable		Workable	
Prototyping Method	Accessible	Scalable	µm-Scale Uniformity	Low Porosity	Flexible	Shapeable
Electrospun Fiber						
Thermally Drawn Fiber						
PVDF Monofilament						
Piezoelectric Ink						
SpaceSkin: Crimped Cable						
SpaceSkin: Coated Cable						

Table 2. Summary of manufacturing methods considered, with green indicating a feature, yellow indicating a potential feature, and grey indicating an unlikely feature for each method

closely with a materials science laboratory to study high performance, thermally drawn piezoelectric fiber in an aerospace context, the results of which will be documented in a separate publication.

2.2 BETA CLOTH DEVELOPMENT AND SPECIFICATION RELATIVE TO COMMERCIAL COUNTERPART

Beta cloth is a densely woven, Teflon-impregnated beta ('BC') fiberglass fabric used as an exposed shell layer on persistent space assets and spacesuits ranging from Apollo era spacesuits to Bigelow Aerospace next generation inflatable habitats. At 4.3 micron diameter, BC filament yarn produces the most flexible commercially available fiber bundle and the resulting fabric is notable for its resilience to atomic oxygen erosion and other aspects of the harsh space environment (for instance, extended particle/UV radiation and thermal cycling). Its high weave density structure protects underlying multilayer insulation coatings from erosion. Most importantly, this material has decades of flight heritage. In coordination with Beta Cloth manufacturer JPS Composites, we manufactured three prototypes closely approximating the properties of NASA-approved material, incorporating weft-inserted piezoelectric fiber sensors pictured in Figure 4.

Commercial Beta cloth (Figure 4, top left) is woven into a tight mat and impregnated in Teflon, which increases the durability and tear resistance of the fabric. A surfactant is added to improve Teflon adhesion, which is subsequently removed during a heat treatment process. Because this heat treatment is likely to depole or otherwise damage piezoelectric fibers, we opted in our principal prototype to source BC fiberglass yarn pre-coated with Teflon from W.F. Lake, forgo Teflon impregnation, and thereby directly weft-insert the sensors during the manufacturing process without any heat treatment required. The resulting fabric (Figure 4, top right) is more porous than an impregnated counterpart. In exchange, the precoated beta fibers do not need further treatment for loom compatibility and are thus a higher quality product. For completeness, a secondary prototype with Teflon impregnation and heat treatment was completed, which also contains removable spacer yarns weft-inserted into the textile allowing sensors to be inserted manually (Figure 4, bottom right). This manufacturing procedure more closely emulates NASA's approved process, yet with the added complexity of hand-insertion of sensors. Because hand insertion is not scalable, we focus primarily on evaluating our primary prototype. Other sensor integration methods may also be feasible.

Finally, a third prototype incorporates Liberator conductive yarn from Syscom Advanced Materials (Figure 4, bottom left) under consideration for hypervelocity impact plasma charge measurements on habitats, capacitive touch detection on spacesuits, and general signal routing across future space-grade e-textiles. Its analysis is ongoing.

2.3 SCALING TO LARGE AREA: LOW POWER READOUT ELECTRONICS

Scaling this system to large areas on the order of tens of meters will ultimately require the following key considerations:

1. Optimize fiber sensor electrical interconnects

Downloaded From: https://www.spiedigitallibrary.org/conference-proceedings-of-spie on 13 May 2020
Terms of Use: https://www.spiedigitallibrary.org/terms-of-use

Sample	**Texture** (yarns/in)	**Thickness** (in)	**Weight** ($yards/lb^2$)	**Filament Diameter** (in)
Commercial Beta Cloth (NASA)	85 x 60	.008	.44	.00017
Teflon Coated Fiberglass Yarn	42 x 35	.01	.56	.0112
BC Yarn, Teflon Impreg., Heat Treated	85 x 60	.014	0.5	.005
Fiberglass + Silvered Vectran Hybrid	42x40	0.01	0.7	.0112 (BC yarn)
.	.	.	.	.0089 (Vectran)

Table 3. Comparison between key textile metrics for commercial Beta cloth vs. modified Beta cloth materials

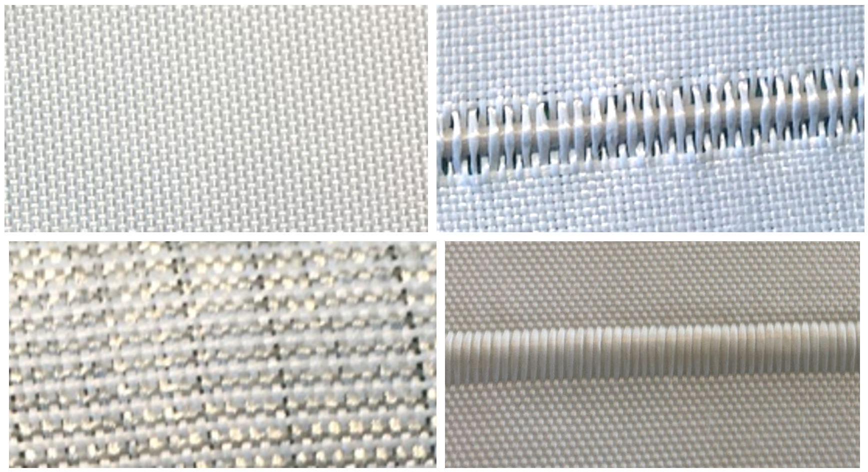

Figure 4. Commercial Beta Cloth (top left) Beta Cloth simulant with weft-inserted piezoelectric fiber (top right) Beta cloth simulant with conductive yarn inserted (bottom left) Teflon impregnated Beta cloth simulant with spacer yarn (bottom right). Other integration strategies may be possible.

2. Improve robustness to noise pickup from long sensors
3. Intelligently parse data from a large number of channels
4. Keep total system power consumption sufficiently low so as to increase adoption rates by representing negligible burden on the spacecraft's total supply.

At this stage of development, we have begun to address (4). We designed ultra-low-power readout electronics using some of the lowest power consumption chips available commercially. The design is broadly summarized in Figure 2.3 and technical details are included in Appendix A. The expected signal duration of an impact is on the order of hundreds of microseconds, necessitating a sampling rate at least on the order of hundreds of kilohertz. The overall read-in topology consists of differential pair inputs fed through an instrumentation amplifier, 2nd order Sallen Key filtering and amplification stages, an ADC, and a microcontroller (MCU). The external ADC is designed to store input data in a circular buffer. The MCU operates in ultra low power mode until signal voltage surpasses a threshold, at which point contents of the circular buffer are stored to memory. The MCU includes both internal as well as supplemental external ferroelectricic RAM (FRAM), robust to radiation-induced bit flipping. An optional low power multiplexer has also been spec'ed for potential use.

While high-level topology of the readout electronics is fairly typical, engineering sophistication lies in optimizing the circuit for stable supply lines, ultra low power consumption and operation at a sufficiently high sampling rate. The best-case-scenario power consumption at 2.2 volts line voltage and with independent channels (no multiplexing) is estimated at 200 μA per channel in active state and 70 μA per channel in sleep state. Therefore, based on calculations informing this low power design, one might expect as a first order approximation a current consumption on the order of tens to hundreds of milliamps for a system that is one day scaled to hundreds of sensors across tens of meters.

Downloaded From: https://www.spiedigitallibrary.org/conference-proceedings-of-spie on 13 May 2020
Terms of Use: https://www.spiedigitallibrary.org/terms-of-use

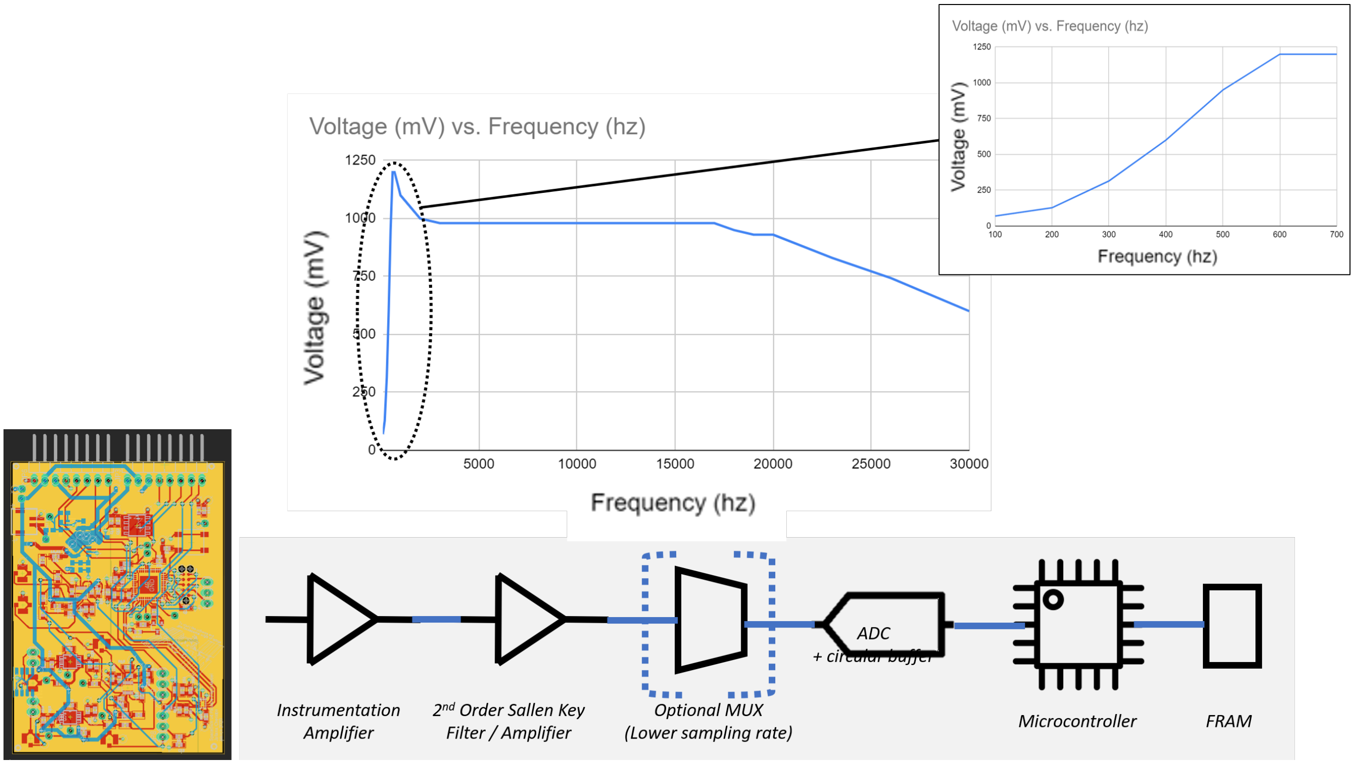

Figure 5. High level Summary of ultra low power readout electronics. PCB Layout (Top left) PCB Transfer function (top right) readout stages (bottom)

3. PROTOTYPE CHARACTERIZATION EXPERIMENTS

To demonstrate a sensate material's protective and sensing capabilities, it is important to characterize both any influence of the sensor on baseline material performance of Beta cloth fabric, as well as to characterize sensor performance for impact detection.

3.1 MATERIAL CHARACTERIZATION

Preliminary material survivability testing is as follows:

(1) **Outgassing in low vacuum**: fiber and fabric samples were placed in a vacuum chamber at 25 inHg pressure for 24 hours at 65°C and 125°C. Samples were weighed at milligram precision before and after vacuum testing. No changes to mass were observed. This test should be repeated under substantially higher vacuum conditions when feasible.

(2) **Thermal emissivity / absorption**: Beta cloth forms the outer layer of temperature regulating multi-layer insulation. Therefore, any effects of of a sensate Beta Cloth on thermal performance should be quantified in order to prove that the material sufficiently preserves its protective properties. An ET100 emissometer with a 0.520-inch sampling port was used to compare commercial Beta cloth's thermal performance to bare Beta cloth replicas and to a Beta cloth replica with a single piezoelectric fiber (constructed using method 1) inserted. The inserted fiber occupied 25% of total aperture. The introduction of 25% fiber by area increased diffuse absorption by around 60%. Since the main operational role of a thermal blanket is to prevent a spacecraft from overheating, there is incentive to either minimize the number of sensors introduced or to apply a white coating. Results are summarized in Table 6.

Downloaded From: https://www.spiedigitallibrary.org/conference-proceedings-of-spie on 13 May 2020
Terms of Use: https://www.spiedigitallibrary.org/terms-of-use

	Thermal Absorption		*Thermal Emissivity*		
	α_{diff}	α_{spec}	ε_{20°	ε_{60°	ε_h
Commercial beta cloth [BENCHMARK]	**.19**	**1.0**	**.92**	**.89**	**.87**
Beta cloth prototype, no sensor	.18	1.0	.92	.89	.86
Beta cloth + single piezoelectric fiber	.32	1.0	.86	.85	.80
Beta cloth replica w/silver coated Vectran	.22	1.0	.58	.57	.58

Figure 6. Summary of emissivity/absorption measurements. Beta cloth prototype closely approximates commercial Beta cloth. The introduction of 25% fiber by area increased diffuse absorption significantly but had only modest effects on emissivity.

3.2 MICROPARTICLE IMPACT TESTING

In addition to testing protective properties of the material using ground facilities, a complementary effort is underway to measure the sensing capabilities of the system. Single particle impact experiments were performed using an all-optical setup for microparticle acceleration under low vacuum conditions, the Laser-Induced Particle Impact Test (LIPIT). The LIPIT has been described in details elsewhere.[15] In short, a laser pulse (10-ns duration, 532-nm wavelength) was focused onto a metallic layer comprised between a glass substrate (210-m thickness) and a polyurea film (30-m thickness). The plasma generated upon laser absorption quickly expanded and deformed the polyurea film. Particles deposited on top of the polyurea film were subsequently accelerated to high velocities. High-velocity particles traveled through a pinhole (200 μm diameter) to block ablation debris and marginal ejected particles (Fig. 3.2a). Particles were imaged as they traveled through the pinhole using a high-speed camera (SIM, Specialised Imaging) (Fig. 3.2b). Particles velocities were measured from recorded image sequences.

Spherical steel microparticles (~7.8g/cc density) were purchased from Cospheric, and spherical silica microparticles (7 and 13.8 μm diameter, 1.85 g/cc density) were purchased from Microparticles GmbH. Prior to launch, particle diameters were measured using a secondary CCD camera. Particles with an average size of 28 μm (+/- 4 μm) were selected and accelerated to speeds ranging from 100 to 900 m/s. Targets were placed about 1 cm away from the pinhole. Experiments were conducted in a vacuum chamber under a pressure of 0.15 mbar (+/- 0.05 mbar).

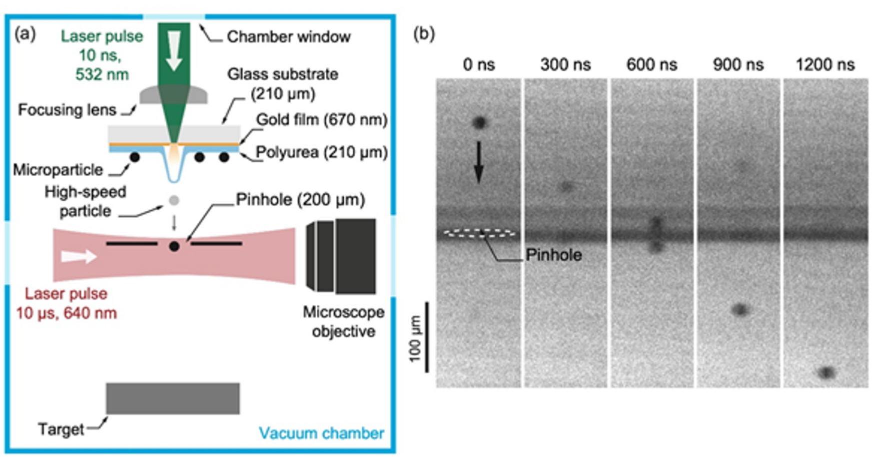

(a) Schematic illustration of the LIPIT setup. (b) Representative image of a steel particle traveling through the pinhole, here at 585 m/s.

Downloaded From: https://www.spiedigitallibrary.org/conference-proceedings-of-spie on 13 May 2020
Terms of Use: https://www.spiedigitallibrary.org/terms-of-use

3.3 IMPACT EXPERIMENT SETUP

Two piezoelectric Beta cloth samples have been tested in the LIPIT facility. The first test used an initial prototype constructed via method 1 (as introduced in Section 2.1). The sample was tested in ambient pressure and temperature conditions using preliminary readout electronics. Setup is pictured in Figure 7a.

The second test was conducted in vacuum condition and with a robust prototype constructed using method two (as introduced in Section 2.1, professional grade fabric, and improved readout electronics. 30-micron steel impactors were used in this initial vacuum testing campaign. Setup internal to the vacuum chamber is pictured in Figure 7b. Careful attention was dedicated to reducing noise introduced by chamber BNC pass-throughs, including storage of all high impedance signal lines inside the chamber and shielding of external cabling using grounded copper mesh.

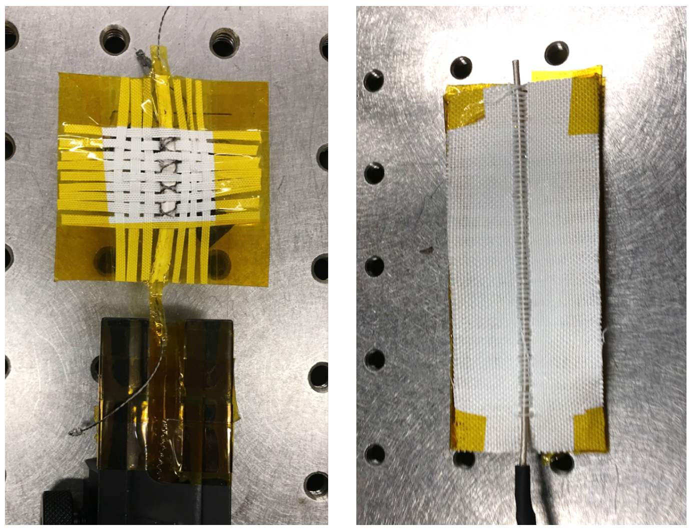

Figure 7. Initial prototype with piezoelectric element constructed using method 2, handwoven into simple fabric and tested in the LIPIT facility under ambient pressure and temperature conditions using preliminary readout electronics (left) Subsequent prototype with piezoelectric element constructed using method 1, integrated into professional grade fabric and tested under vacuum condition and with readout electronics as described in Section 2.3(right)

4. IMPACT TESTING RESULTS

Linear fit between impactor velocity and integrated voltage, as well as impactor velocity and peak-to-peak voltage, is observed with varying degrees of certainty. linear fits for tests conducted under ambient condition are shown in Figure 4 and tests under vacuum condition are shown in Figure 12. Note that since both the design of readout electronics and design of fabric sample changed significantly between trials, these results should not be directly compared.

As the velocity of steel particles increase, so too does the standard deviation in features of the measured impactor signature. It is important to note that the nature of impact may vary significantly. Microscope images shown in Figure 10 demonstrate preliminary evidence that whereas particles that strike the fabric or one of the warp yarns holding the sensor in place may adhere, particles directly striking the sensor tend to rebound off of the sensor and leave a crater. Further, due to the curved surface of the cylindrical cross section sensor, particle impacts at different locations along the width of the sensor will exert varying stress vectors on the piezoelectric domain of the sensor for the same impactor velocity.

Evidence for the excitation of varying modes is visible in spectral analysis - some impacts excite broadband pulses whereas others show greater spectral energy in narrowband regions. It may well be that impactors striking and rebounding off of the rigid sensor body register as pulses, whereas strikes on either warp yarn holding the sensor or on fabric adjacent to sensor excite modes of either the fabric or the sensor. Figures 11 and 12 show

Downloaded From: https://www.spiedigitallibrary.org/conference-proceedings-of-spie on 13 May 2020
Terms of Use: https://www.spiedigitallibrary.org/terms-of-use

examples of differing spectral classes for each of the two impact testing campaigns conducted in time domain and frequency domain (via Wavelet transform). The Wavelet representation is used in order to achieve improved frequency resolution for high frequency signal components with short time duration. Follow-on work will consist of developing a more robust physical understanding of the impactor signature classes.

The impactor size regime considered in this testing campaign is microscopic compared to the sensor width, and unlikely to fully disable the sensor. However, a larger impactor could cause enough damage to take out a sensor line, providing a further case for sparseness.

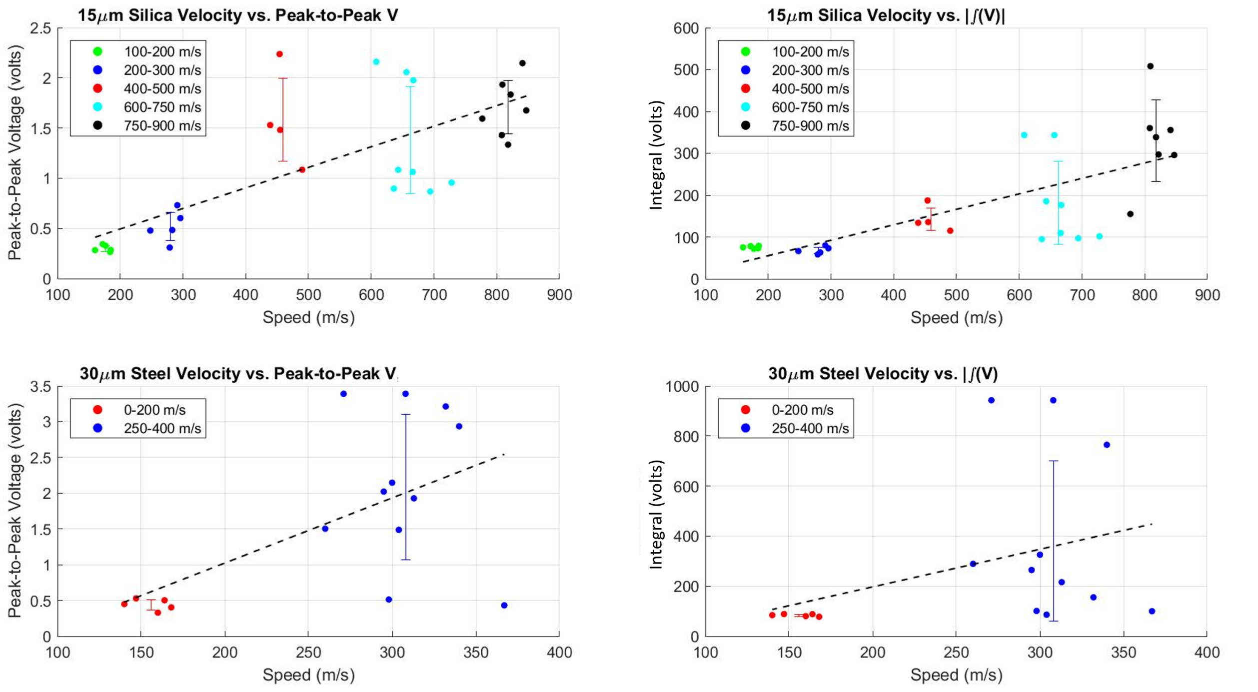

Figure 8. Integral and peak-to-peak measurements for silica and steel particles striking piezoelectric fiber under ambient conditions

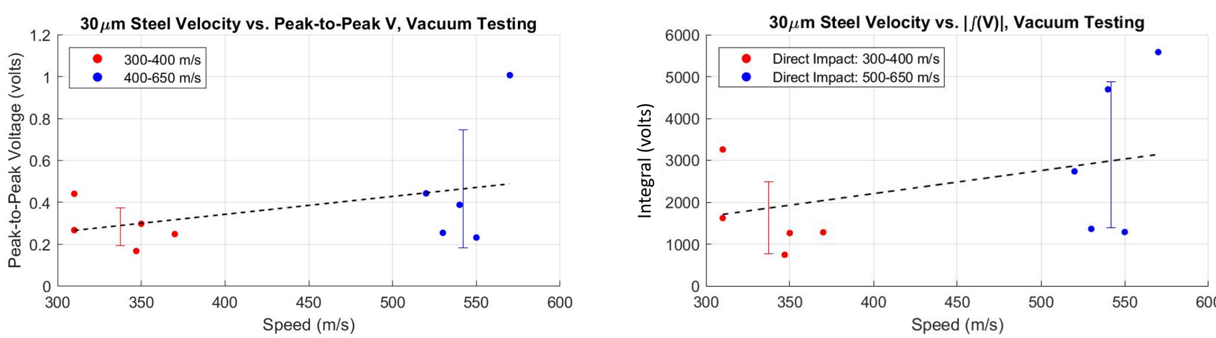

Figure 9. Integral and peak-to-peak measurements for steel particles striking piezoelectric fiber under vacuum condition

Downloaded From: https://www.spiedigitallibrary.org/conference-proceedings-of-spie on 13 May 2020
Terms of Use: https://www.spiedigitallibrary.org/terms-of-use

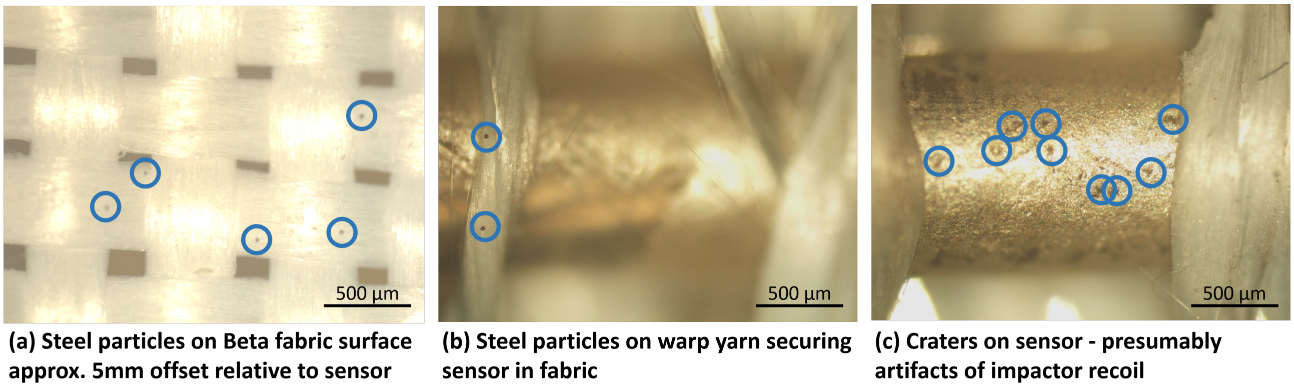

Figure 10. Location of impact, with either steel particles or craters indicated on (a) fabric (b) warp yarn on sensor (c) direct sensor impact

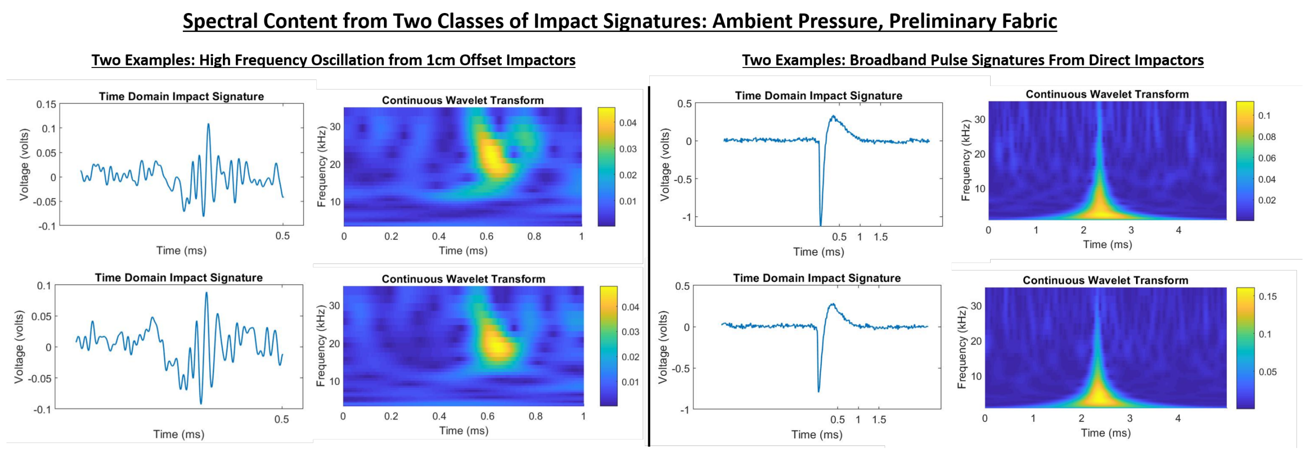

Figure 11. Pairs of examples for two spectral classes under ambient condition, showing time and frequency domain representations. Left two impact signatures are representative of 1cm offset impactor signatures, and right two plots are representative of direct impact signatures

5. PREPARATION OF SAMPLES FOR 2020 DEPLOYMENT ON INTERNATIONAL SPACE STATION

With logistical support from Space BD Inc., we are deploying passive fabric samples for one year on the ExHAM external facility of the International Space Station. The exposure period will allow for post-flight characterization of material resilience to the space environment including (1) quantification of atomic oxygen erosion, (2) microscope/multi-spectral imaging of radiation-induced degradation and coloring, (3) measurement of depoling or other effects on sensor performance induced by thermal cycling (4) effects on circuit board functioning induced by radiation. A schematic and image of the deployment setup is shown in Figure 13.

6. CONCLUSION

We have reported the detailed technical development of the first aerospace electronic textile, with emphasis on piezoelectric fiber, aerospace-grade fabric, and low power electronics prototyping. Samples prepared for deployment on the International Space Station are described. High-velocity impact data shows first evidence of a correlation between the impactor speed and the energy contained in the resulting signature. Variations in spectral content of impactor response suggests varying excitation modes depending on the nature of impact, which will be studied more carefully in follow-on work. We are also studying various protective coatings to further shield sensors from atomic oxygen degradation and thermal cycling.

Downloaded From: https://www.spiedigitallibrary.org/conference-proceedings-of-spie on 13 May 2020
Terms of Use: https://www.spiedigitallibrary.org/terms-of-use

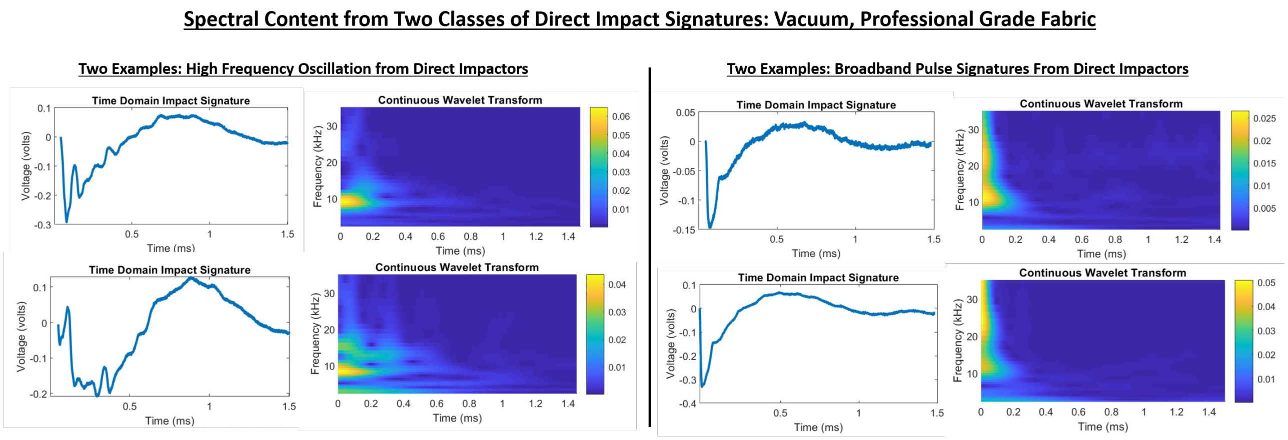

Figure 12. Pairs of examples for two spectral classes under vacuum condition, showing time and frequency domain representations. Left two impact signatures are representative one class of direct impactor signatures containing high frequency narrowband oscillatory component, and right two plots are representative of a second class of direct impact signatures consisting of broadband pulse

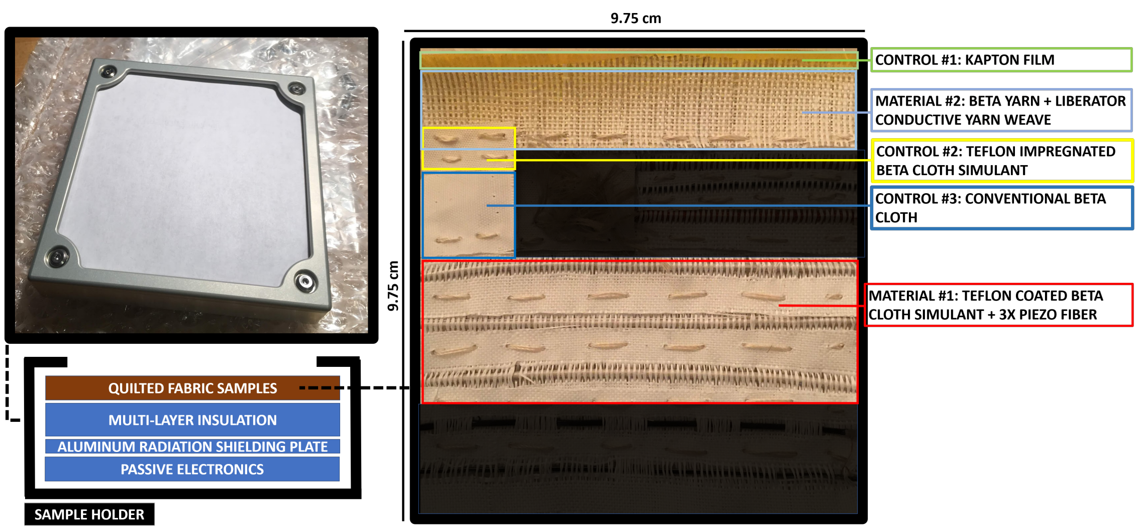

Figure 13. Graphics showing overall planned 2020 deployment setup for fabric swatches and passive electronics on International Space Station ExHAM Exposure Facility

7. ACKNOWLEDGEMENTS

Thank you to Daisuke Takahashi and the rest of Space BD as well as to the Japanese Space Agency (JAXA) for working with our team to coordinate the launch of SpaceSkin samples to the ExHAM facility on the International Space Station. Thank you to the R&D team at JPS Composites for manufacturing professional grade fabric samples for high fidelity comparison to NASA-approved material. Funding for this research and for our international collaboration has been provided by the MIT Misti Hayashi Ulvac Seed Fund, NASA TRISH, MIT Media Lab Space Exploration Initiative, and the MIT Media Lab consortium fund. This material is based upon work supported, in part, by the U.S. Army Research Office through the Institute for Soldier Nanotechnologies, under Cooperative Agreement Number W911NF-18-2-0048. LIPIT upgrades were funded by JSPS KAKENHI Grant Number JP 18KK0128.

Downloaded From: https://www.spiedigitallibrary.org/conference-proceedings-of-spie on 13 May 2020
Terms of Use: https://www.spiedigitallibrary.org/terms-of-use

8. APPENDIX A: KEY ELECTRONICS SPECIFICATIONS

Key Board Specifications		
Supply Voltage	2.2	Volts
Bandwidth	30	kHz
Min Resolvable frequency	500	Hz
Gain	100	
Target sampling rate	240	kHz
Expected signal duration	500	µS
Total # of samples based on expected signal duration	125	

Key ADC Specifications (ADS7142)		
T_hso	50	ns
tconv + tacq	1.05	µS
Oscillator frequency	20	MHz
nCLK for sampling frequency	83	
Total pre-trigger data	48	µS
Sampling time	4	µS
MCU wakeup time	7	µS
Data lost during MCU wakeup	2 x 4	µS

Key MUX Specifications (TMUX1108)		
Charge Injection	1	pC
Transition time between channels	14	Ns
Step response settling: INA333 (small signal)	10	µS
Step response settling: INA333 (large signal)	100	µS
Step response settling: MIC863	15	µS
Max sampling frequency assuming small INA333 signal + 15 µS MIC863 settling time	70	kHz

Key Power Specifications			
	Quiescent Current (µA)	**Bandwidth@10x gain (kHz)**	**CMRR (dB)**
INA333 Instrumentation amplifier	50	35	115
MIC861 operational amplifier	4.6	40	77
	Quiescent Current (µA)	**Current in Low Power Mode (µA)**	**Speed**
ADS7142 ADC	0.4 (900 nW/chan)		140 ksps
MSP430FR5969 MCU	100 (100 µA/MHz)	0.4	
MB85RC1MT FRAM	15 (standby)	4 (sleep)	1MHz-3.4Mhz

Figure 14. Detailed specifications for Ultra Low Power Electronics

REFERENCES

[1] Barbeau, C. and Cochran, R., "Textile material for outer shell of firefighter garment," (Apr. 5 1994). US Patent 5,299,602.

[2] Jones, C., Lawson, C., Ayres, D., et al., "Geotextile reinforced piled embankments," *Geotextiles, Geomembranes and Related Products, Den Hoedt (ed.)* , 155–160 (1990).

[3] Cherston, J. and Paradiso, J. A., "Spaceskin: development of aerospace-grade electronic textile for simultaneous protection and high velocity impact characterization," in [*Sensors and Smart Structures Technologies for Civil, Mechanical, and Aerospace Systems 2019*], **10970**, 109700J, International Society for Optics and Photonics (2019).

[4] Scott, R. A., [*Textiles for protection*], Elsevier (2005).

[5] Chapman, R., [*Smart textiles for protection*], Elsevier (2012).

[6] Cherston, J. and Paradiso, J. A., "Space webs as infrastructure for crawling sensors on low gravity bodies," (2017).

[7] Cherston, J., Strohmeier, P., and Paradiso, J. A., "Grappler: Array of bistable elements for pinching net-like infrastructure to low gravity bodies," in [*AIAA Scitech 2019 Forum*], 0871 (2019).

[8] Xu, Y., Tai, Y.-C., Huang, A., and Ho, C.-M., "Ic-integrated flexible shear-stress sensor skin," *Journal of Microelectromechanical Systems* **12**(5), 740–747 (2003).

[9] Ikari, S., Fujiwara, M., Kondo, H., Matsushita, S., Yoshikawa, I., Yoshioka, K., Hikida, R., Kawabata, Y., Nakajima, S., Funase, R., et al., "Solar system exploration sciences by equuleus on sls em-1 and science instruments development status," (2019).

[10] Burchell, M. J., "Panspermia today," *International Journal of Astrobiology* **3**(2), 73–80 (2004).

[11] Nilsson, E., Lund, A., Jonasson, C., Johansson, C., and Hagström, B., "Poling and characterization of piezoelectric polymer fibers for use in textile sensors," *Sensors and Actuators A: Physical* **201**, 477–486 (2013).

[12] Hadimani, R. L., Bayramol, D. V., Sion, N., Shah, T., Qian, L., Shi, S., and Siores, E., "Continuous production of piezoelectric pvdf fibre for e-textile applications," *Smart Materials and Structures* **22**(7), 075017 (2013).

[13] Krajewski, A. S., Magniez, K., Helmer, R. J., and Schrank, V., "Piezoelectric force response of novel 2d textile based pvdf sensors," *Sensors Journal, IEEE* **13**(12), 4743–4748 (2013).

Downloaded From: https://www.spiedigitallibrary.org/conference-proceedings-of-spie on 13 May 2020
Terms of Use: https://www.spiedigitallibrary.org/terms-of-use

[14] Egusa, S., Wang, Z., Chocat, N., Ruff, Z., Stolyarov, A., Shemuly, D., Sorin, F., Rakich, P., Joannopoulos, J., and Fink, Y., "Multimaterial piezoelectric fibres," *Nature materials* **9**(8), 643 (2010).

[15] Veysset, D., Sun, Y., Kooi, S. E., Lem, J., and Nelson, K. A., "Laser-driven high-velocity microparticle launcher in atmosphere and under vacuum," *International Journal of Impact Engineering* **137**, 103465 (2020).

Downloaded From: https://www.spiedigitallibrary.org/conference-proceedings-of-spie on 13 May 2020
Terms of Use: https://www.spiedigitallibrary.org/terms-of-use